lncRNA TINCR promotes the development of cervical cancer via the miRNA-7/mTOR axis *in vitro*

XUAN LIU[1], CUI XIA WANG[2], QIN FENG[3] and TAO ZHANG[4]

[1]Department of Gynecology, Women and Children's Hospital, Qingdao University; [2]Department of Pediatrics, Eighth People's Hospital of Qingdao Shandong; Departments of [3]Imaging, and [4]General Internal Medicine, Women and Children's Hospital, Qingdao University, Qingdao, Shandong 266000, P.R. China

Received March 16, 2023; Accepted June 9, 2023

DOI: 10.3892/etm.2023.12186

Abstract. The present study aimed to examine the effects of the long non-coding (lnc)RNA expressed by tissue differentiation-inducing non-protein coding RNA (TINCR) on cervical cancer development. For this purpose, adjacent normal and cancer tissues were obtained from patients with cervical cancer and the lncRNA TINCR level was examined using reverse transcription-quantitative PCR (RT-qPCR) and *in situ* hybridization. The association between lncRNA TINCR and the clinicopathological characteristics and prognosis of patients with cervical cancer was also analyzed. Furthermore, the expression levels of lncRNA TINCR, miRNA-7, mTOR, hypoxia-inducible factor 1 subunit α and VEGF were measured using RT-qPCR and western blot analysis. Cell proliferation, apoptosis, and invasion and migration were examined using MTT assay, 5-ethynyl-2'-deoxyuridine staining, flow cytometry, TUNEL assay, and Transwell and wound healing assays. The association between lncRNA TINCR, miRNA-7 and mTOR was also examined using a luciferase assay. The results revealed that the lncRNA TINCR level was significantly increased in cervical cancer tissues and was associated with the overall survival of patients (low vs. high expression group; P=0.0391). LncRNA TINCR was also associated with the clinicopathological characteristics of patients with cervical cancer. Following the knockdown of lncRNA TINCR using small interfering (si)RNA, cell proliferation was significantly decreased and cell apoptosis was significantly increased (P<0.001 for both); cell invasion and migration were also significantly decreased (P<0.001 for both) following transfection with mimics miRNA-7. Transfection with miRNA-7 antisense oligonucleotide decreased the antitumor effects of si-TINCR in Siha and HeLa cell lines. As shown using the dual-luciferase assay, lncRNA TINCR could target miRNA-7 and miRNA-7 could directly regulate mTOR in HeLa and SiHa cell lines. In conclusion, the present study demonstrated that lncRNA TINCR could promote cervical cancer development via regulation of the miRNA-7/mTOR axis *in vitro*.

Correspondence to: Dr Tao Zhang, Department of General Internal Medicine, Women and Children's Hospital, Qingdao University, 6 Tongfu Road, Shibei, Qingdao, Shandong 266000, P.R. China
E-mail: zhangtao230309@163.com

Key words: lncRNA TINCR, cervical cancer, HeLa, SiHa, miRNA-7, mTOR

Introduction

Among the malignant tumors of the female reproductive system, the incidence rate of cervical cancer is second only to breast cancer, which poses a severe threat to women's health (1). The 5-year survival rate of patients with cervical cancer in several underdeveloped countries is <50% (2). With advancements being made in medicine, cervical cancer treatment has gradually changed from single surgical treatment to a combination of traditional and neoadjuvant treatments; however, the prognosis of patients has not been markedly improved and the mortality rate remains high (3). Long non-coding RNAs (lncRNAs) are non-coding RNAs with a length of >200 nt, which cannot encode proteins but can regulate gene expression through transcriptional, post-transcriptional and epigenetic mechanisms (4). Relevant studies demonstrated that the lncRNA tissue differentiation-inducing non-protein coding RNA (TINCR) participates in tumor progression and is abnormally expressed in various tumor tissues (5-8). TINCR plays an inhibitory role in prostate cancer (5), whereas it plays a promoting role in other types of tumors including NSCLC, HCC and colon cancer, TINCR is closely correlation with poor prognosis in NSCLC and colon cancer and TINCR overexpression also stimulated cancer cells biological activities including cell proliferation, invasion and migration (6-8). However, the expression of lncRNA TINCR in cervical cancer and its association with the prognosis of patients, as well as its mechanisms of action in cervical cancer occurrence and development remain unclear.

It was demonstrated that lncRNAs may play a role in tumor occurrence and development by regulating the expression of relevant micro(mi)RNAs (9-12). miRNAs are endogenous short-chain RNAs, which can specifically bind to complementary sites in the 3' untranslated region (3'-UTR) of the target mRNA and inhibit its translation or promote its degradation, thus regulating target gene level at the post-transcriptional

level. According to a previous study, several miRNAs are abnormally expressed in cancer (13-15). For example, the over-expression of miR-17-5p was shown to promote the malignant proliferation of tumor cells by suppressing E2F transcription factor 1 expression (14); miR-145 was shown to inhibit tumor cell growth by targeting MAPK to exert an anti-carcinogenic effect (15). miRNA-7 is a key member of the miRNA family (16-18). Previous studies confirmed that abnormal miRNA-7 level is closely related to cancer occurrence (16-18). However, it is not yet clear whether miRNA-7 may play a role in the regulation of cervical cancer biological activity through TINCR.

On this basis, in the present study, TINCR was first detected in cervical cancer and normal para-cancerous tissues using *in situ* hybridization (ISH) and reverse transcription-quantitative PCR (RT-qPCR), and the associations between the TINCR level and the pathology and prognosis of patients with cervical cancer were analyzed. Additionally, the effects of TINCR knockdown on cervical cancer cell biological activities were examined and the corresponding molecular mechanisms were examined *in vitro*.

Materials and methods

Clinical data. A total of 40 patients with cervical cancer undergoing surgical resection at the Women and Children's Hospital, Qingdao University (Qingdao, China) from September 2015 to May 2017 were selected as subjects, aged 32-70 years, with an average age of (54.682±12 27) years. The resected cancer tissues were used as the experimental group, while the para-cancerous tissues (>2 cm from the tumor margin) from the same patients were used as the control group. The inclusion criteria were as follows: i) Confirmed diagnosis of cervical cancer by a pathological examination; ii) receiving no radiotherapy or chemotherapy 3 months before surgery; iii) complete clinical and pathological data; and iv) informed consent provided by patients and their families. The exclusion criteria included the following: i) Presence of other malignant tumors; ii) complications such as hepatic, renal and cardiac dysfunctions; iii) autoimmune diseases; and iv) pregnant and lactating women.

Depending on the International Federation of Gynecology and Obstetrics (FIGO) staging criteria, the subjects were divided into stage I-II (n=18) and stage III-IV (n=22). There were 16 patients with adenocarcinoma and 24 with squamous cell carcinoma. Among all patients, 18 patients presented with and 22 without lymph node metastasis. A total of 17 patients presented with a myometrial invasion depth >1/2 and 23 with a myometrial invasion depth ≤1/2. All the patients were followed up for 5 years from the date of the pathological diagnosis to 1 June 2022, to record their survival status, without the loss of any patients. The present study was approved by the Ethics Committee of Women and Children's Hospital, Qingdao University (approval no. 2015081305).

Sample collection. The cervical cancer tissues resected surgically were collected as the experimental group. Additionally, para-cancerous tissues >2 cm from the tumor margin were collected as the control group. The collected samples were divided into two parts. One was embedded in paraffin for hematoxylin and eosin (H&E) staining and ISH, and the other was stored in a refrigerator at -80˚C for later use.

Measurement of TINCR levels in tissues using ISH. To measure the lncRNA TINCR levels in cervical cancer and normal para-cancerous tissues, ISH was performed as per the instructions provided with the relevant kit (Boster Biological Technology). Digoxin-labeled lncRNA TINCR probe (Boster Biological Technology; cat. no. MK10932; 1:400) was added to the paraffin-embedded tissue sections (5 μm) for incubation at 55˚C for 1 h, followed by washing by PBS. Subsequently, the tissues were sealed in 0.2xSSC (Sigma-Aldrich; Merck KGaA) solution at 60˚C for 1 h. After removing the reagents, the tissue sections were placed in TBST containing anti-digoxin antibody (1:200; cat no. ab30512, Abcam), followed by incubation at 37˚C for 1 h. Finally, the sections were stained at room temperature with H&E (cat. no. KGA224; Nanjing KeyGen Biotech Co., Ltd.) for 2 h and observed and photographed under an optical microscope (CX23; Olympus Corporation).

Materials and reagents. The HeLa and Siha (lncRNA TINCR expression was most upregulated in Hela and Siha cell lines; Fig. S1) cells were purchased from The Cell Bank of Type Culture Collection of the Chinese Academy of Sciences. FBS, DMEM/F12 (HyClone; Cytiva), TRIzol™ reagent, Lipofectamine 2000™ (cat. no. 11668-019), RIPA lysate and the BCA protein quantitative kit were from Invitrogen (Thermo Fisher Scientific, Inc.). The Annexin V-FITC/PI cell apoptosis kit was obtained from CapitalBio Technology, Inc. Matrigel was obtained from BD Biosciences. The MTT assay kit and Transwell chambers were obtained from MilliporeSigma. The dual-fluorescent enzyme detection kit was purchased from Promega Corporation. The mTOR (1:500; cat. no. ab134903), hypoxia-inducible factor 1 subunit α (HIF-1α; 1:500; cat. no ab.51608), anti-VEGF (1:500; cat. no. ab32152) and anti-GAPDH (1:500; cat. no. ab8245) antibodies were obtained from Abcam.

RT-qPCR assay. Total RNA was extracted from cells or tissues using the TRIzol reagent and reverse transcribed into cDNA with a SuperScript™ VILO™ cDNA Synthetic reagent kit (Thermo Fisher Scientific, Inc.; cat. no. 11754050), according to the manufacturer's instructions. Subsequently, qPCR was then performed using the SYBR-Green PCR Kit (Takara Biotechnology Co., Ltd.; cat. no. DRR041A). The RT-PCR conditions were as follows: Initial denaturation at 95˚C for 10 min, followed by 40 cycles of denaturation at 95˚C for 5 sec, annealing at 60˚C for 30 sec and elongation at 72˚C for 32 sec. The primers used for RT-qPCR are presented in Table I. U6 was used as the internal reference for miRNA-7 and GAPDH for the other genes. RNA expression levels were quantified using the $2^{-\Delta\Delta Cq}$ method (19).

Cell culture and transfection. The HeLa and SiHa cells were cultured in DMEM/F12 supplemented with 10% FBS and placed in an incubator a 37˚C with 5% CO_2. When cell confluence reached 70-80%, the cells were digested with 0.25% trypsin (Sigma-Aldrich; Merck KGaA) and centrifuged at 800 x g for 5 min at room temperature. After discarding the supernatant, the cells were resuspended in PBS and adjusted

Table I. Primer sequences used for quantitative PCR.

Gene name	Forward	Reverse
TINCR	5'-TGTGGCCCAAACTCAGGGATACAT-3'	5'-AGATGACAGTGGCTGGAGTTGTCA-3'
miRNA-7	5'-ACGTTGGAAGACTAGTGATTT-3'	5'-TATGGTTGTTCTGCTCTCTGTCTC-3'
mTOR	5'-CGTCAGCACCATCAACCTCCAA-3'	5'-TCAGCCGTCTCAGCCATTCCA-3'
Hypoxia-inducible factor 1 subunit α	5'-GGCGCGAACGACAAGAAAAAG	5'-CCTTATCAAGATGCGAACTCACA-3'
VEGF	5'-CAGCGCAGCTACTGCCATCCAATCG AGA-3'	5'-GCTTGTCACATCTGCAAGTACGTTCGT TTA-3'
U6	5'-TCGCTTCGGCAGCACATATACTAA-3'	5'-AATATGGAACGCTTCACGAATTTGC-3'
GAPDH	5'-AGGCCGGATGTGTTCGC-3'	5'-CATGGTTCACACCCATGACG-3'

to a cell density of $5x10^5$/ml. The cell suspension (1 ml) was collected and seeded in a six-well culture plate, which was placed overnight in an incubator under the same conditions as those described above. After the cells had fully adhered to the wall, the culture medium was removed for transient transfection. The cervical cancer cells were transfected with small interfering (si)-negative control (NC) (cat. no. 12935200; Thermo Fisher Scientific, Inc.), si-TINCR (cat. no. AM16708; Thermo Fisher Scientific, Inc.), miRNA-7 antisense oligonucleotide (ASO) as miRNA-7 inhibitor (5'-ACAACAAAA UCACUAGUCUUCCA-3') and ASO-NC (5'-CAGUACUUU UGUGUAGUACAA-3') at a final concentration of 50 nmol/l, according to the instructions provided with the Lipofectamine 2000 reagent, and incubated under the aforementioned conditions. After 4 h, the culture medium was replaced with DMEM/F12 supplemented with 15% FBS and the transfection efficiency was examined. The cells were photographed and recorded under an X71 (U-RFL-T) fluorescence microscope (Olympus Corporation). Lipofectamine 2000 reagent was used to transfect 10 nM vectors into $6x10^5$ cells according to the manufacturer's instructions. The incubation of the cells with vectors was performed for 48 h at 37˚C. The transfection rates of lncRNA TINCR and miR-7 are shown in Fig. S2.

MTT assay. Following the corresponding treatments for 48 h, the cells in each group were adjusted to a cell density of $5x10^3$ cells/ml, seeded in a 96-well plate with 200 μl DMEN/F12 culture medium supplemented with 10% FBS in each well and then cultured in an incubator at 37˚C with 5% CO_2. After 48 h, the cells were collected and 20 μl MTT was added (5 mg/m1/well), followed by incubation at 37˚C for 4 h. After discarding the original culture medium, the cells were supplemented with DMSO (150 μl/well) and fully shaken at room temperature for 10 min to completely dissolve the formed purple formazan crystals. The absorbance at 450 nm was measured using a microplate reader (Thermo Fisher Scientific, Inc.).

5-ethynyl-2'-deoxyuridine (EdU) staining. Following the corresponding treatments for 48 h, the cells in each group were supplemented with 10 μmol/l EdU, according to the instructions provided with the EdU fluorescent staining cell proliferation kit (cat. no. KGA337; Nanjing KeyGen Biotech Co., Ltd.). Following incubation for 2 h at room temperature, the EdU not infiltrating the DNA was washed with PBS and 4% polyformaldehyde was added to fix the cells for 30 min at room temperature. Subsequently, the fixation solution was washed with PBS and Apollo dye solution (Sigma-Aldrich; Merck KGaA) was added to the cells for incubation in the dark at room temperature for 30 min. The dye solution was washed with PBS and the nuclei were stained with 10 μmol/l DAPI for 5 min at room temperature. Fluorescence images of five randomly-selected fields were obtained under an IX73 fluorescence microscope (Olympus Corporation) and the EdU-positive cells were counted using ImageJ software v1.46 (National Institutes of Health).

Detection of apoptosis using flow cytometry. Following the corresponding treatments for 48 h, the cells in each group were routinely digested with 0.25% trypsin, followed by washing with PBS three times and centrifugation at 800 x g for 5 min at 4˚C. After the supernatant was discarded, the cell concentration was adjusted to $5x10^5$ cells per sample and 195 μl Annexin V-FITC binding buffer was added to resuspend the cells. Subsequently, 5 μl Annexin V-FITC and 10 μl PI were added followed by incubation in the dark at room temperature for 30 min. Apoptosis analysis was performed using a BD FACScan™ flow cytometer with BD CellQuest(TM) software version 5.1 (BD Biosciences).

TUNEL staining. Following the corresponding treatments for 48 h, the cells in each group were fixed with 4% paraformaldehyde (Nanjing KeyGen Biotech Co., Ltd.) at room temperature for 30 min and then incubated at room temperature for 5 min with enhanced immunostaining permeabilization buffer (Nanjing KeyGen Biotech Co., Ltd., cat. no. KGIHC010). The cells were then stained with TUNEL (cat. no. KGA702-1; Nanjing KeyGen Biotech Co., Ltd.) and incubated in the dark at 37˚C for 60 min to observe cell apoptosis under an Olympus IX71 fluorescence microscope (Olympus Corporation). Red fluorescence indicated TUNEL-positive cells.

Transwell assay for cell invasion. Following the corresponding treatments for 48 h, the cells in each group were digested with trypsin and centrifuged (800 x g at 4˚C for 30 sec). The cells were collected and counted using a cell counter (Beckman

Coulter). After adjusting the cell count with serum-free medium, Precoat Matrigel at room temperature for 1 h, the cells were seeded into the upper chamber of Transwell plates at $5x10^4$ cells/well (200 μl/well). The lower chamber was supplemented with 700 μl complete medium to induce the migration of tumor cells and placed in an incubator for 24 h at room temperature. Subsequently, the upper chamber was removed and washed with PBS twice after the supernatant was discarded; the cells that did not pass through the inner side of the upper chamber were wiped off using a cotton swab. Following fixation with 4% polyformaldehyde for 15 min at room temperature, the chambers were rinsed with PBS twice and the cells were stained with crystal violet (Nanjing KeyGen Biotech Co., Ltd.) staining solution for 15 min at room temperature, followed by rinsing with PBS five times. After drying, the cells were observed and photographed under an X71 (U-RFL-T) fluorescence microscope (Olympus Corporation; magnification, x200) and five randomly-selected fields were used to count the number of migrating cells.

Wound healing assay for cell migration. Following the corresponding treatments for 48 h, the cells in each group were digested with trypsin and centrifuged (800 x g at 4˚C for 30 sec). The cells were then resuspended in culture medium supplemented with 5% (w/w) FBS and the cell concentration was adjusted using a cell counter by serum-free medium. Subsequently, the cells were seeded in a six-well plate at $2x10^5$ cells/well (2 ml/well). When the cell density reached 80-90%, the culture medium in the plate was discarded and a vertical line was scratched using a 20 μl pipette tip under a X71 (U-RFL-T) fluorescence microscope (Olympus Corporation; magnification, x100). The cells were then rinsed with PBS twice to remove any residual cells. The changes in cell migration were observed at 0, 24 and 48 h in each group and photographed under an inverted X71 (U-RFL-T) fluorescence microscope (Olympus Corporation; magnification, x100), and the average wound healing rate was analyzed and calculated.

Western blot analysis for relative protein expression in cells. Following the corresponding treatments for 48 h, the cells in each group were collected and centrifuged (800 x g at 4˚C for 30 sec). After the supernatant was discarded, the cells were lysed with radioimmunoprecipitation buffer (Nanjing KeyGen Biotech Co., Ltd.). Following centrifugation (1,000 x g at 4˚C for 45 sec), the supernatant was collected and the total protein content in the supernatant was determined using the BCA method. Proteins were separated by SDS-PAGE on 12% gel and transferred to a PVDF membrane using the wet transfer method. Subsequently, the membranes were blocked using 5% skimmed milk powder at room temperature for 2 h and washed with TBST five times for 10 min each time. The membrane was then incubated with primary antibodies (all from Abcam) against mTOR (1:500; cat. no. ab134903), HIF-1α (1:500; cat. no ab.51608;), anti-VEGF (1:500; cat. no. ab32152) and anti-GAPDH (1:500; cat. no. ab8245) overnight at 4˚C. Following primary incubation, the membrane were washed five times with TBST, 10 min each time and incubated with HRP-conjugated secondary antibodies (1:10,000; Nanjing KeyGen Biotech Co., Ltd., cat. no. KGP1201) at room temperature for 2 h. The membrane was then washed with TBST five times, 10 min each time. Protein bands were visualized using an ECL reagent (Nanjing KeyGen Biotech Co., Ltd.) and a gel imaging system (SYNGENE G:BOX Chemi XR5; Syngene), the gray value of the bands was quantified using ImageJ software v1.46 (National Institutes of Health) and the protein expression levels were normalized to the GAPDH reference gene.

Bioinformatics analysis and dual-luciferase reporter gene assay. Bioinformatics analysis was performed using TargetScan version 7.1 (www.targetscan.org). To clarify the association between TINCR and miRNA-7, the mutant miRNA-7 binding site of TINCR was generated using the quick-change site-directed mutagenesis kit (Stratagene; Agilent Technologies, Inc.). The wild-type (WT) or mutant-type (MT) TINCR was subcloned into the dual-luciferase target vector by Lipofectamine 2000™ (Promega Corporation) to produce the WT or MT TINCR luciferase report plasmid, respectively. To clarify the association between miRNA-7 and mTOR, the MT miR-7 binding site of the mTOR 3'-UTR was generated using the quick-change site-directed mutagenesis kit (Stratagene; Agilent Technologies, Inc.). The WT, MT or luciferase report plasmid was produced. As aforementioned, the cells were co-transfected with miRNA-7 mimics (10 ng/ml) (5'-UGG AAGACUAGUGAUUUUGUUGU-3') or its NC (miRNA-NC) (10 ng/ml; 5'-CAGUACUUUUGUGUAGUACAA-3'), WT (or MT) TINCR reporter plasmid, WT (or MT) MT or 3'-UTR reporter plasmid using the Lipofectamine 2000 reagent. Following cell transfection for 48 h at room temperature, the luciferase activity was detected using a dual-luciferase report assay system (Promega Corporation). Firefly luciferase activity was normalized to *Renilla* luciferase activity.

Statistical analysis. All data were analyzed using SPSS 24.0 software (IBM Corp.). Continuous data are presented as the mean ± standard deviation and were analyzed using one-way analysis of variance with Tukey's post hoc test. Enumeration data are presented as number and were analyzed using chi-square or Fisher's exact test. A Kaplan-Meier curve was used to draw the survival curve of patients with cervical cancer and Cox multivariate analysis was used to analyze risk factors affecting cervical cancer. All statistical tests were two-tailed and $P<0.05$ was considered to indicate a statistically significant difference. All the experiments were performed in triplicate.

Results

Pathological changes and TINCR expression in tissues. H&E staining revealed the pathological differences in the cervical cancer tissues were blur, with tissue infiltration (Fig. 1A). RT-qPCR (Fig. 1B) and ISH (Fig. 1C) revealed that the expression level of lncRNA TINCR in the cervical cancer tissues was significantly higher compared with that in normal tissues ($P<0.001$).

Association between the lncRNA TINCR level and the clinicopathological characteristics of patients with cervical cancer. The 40 patients with cervical cancer included in the present study were divided into the high and low expression groups using the median as cut-off value. The lncRNA TINCR

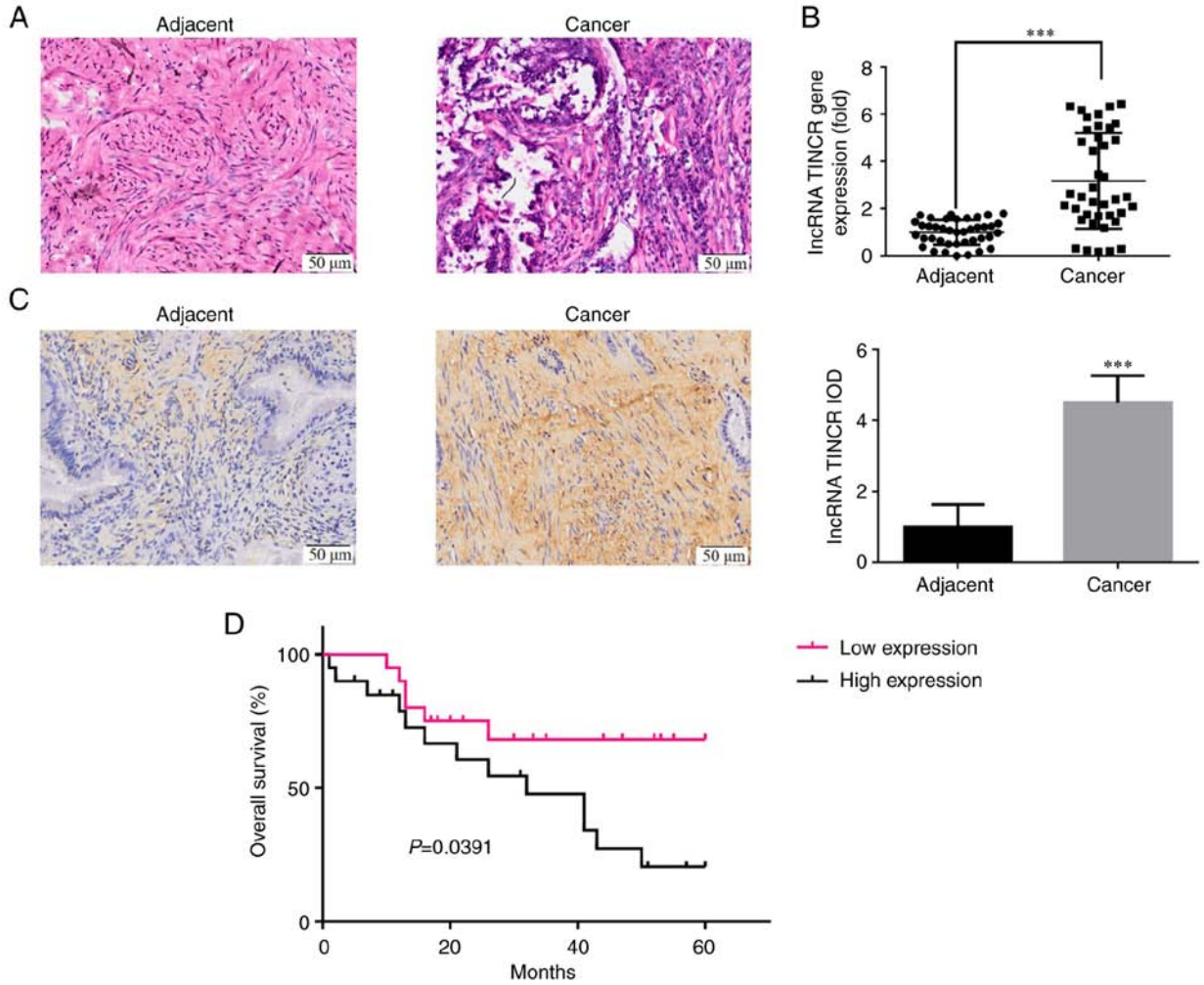

Figure 1. Pathological changes and lncRNA TINCR expression in tissues. (A) Pathological differences in tissues were examined using H&E staining (magnification, x200). (B) LncRNA TINCR expression in tissues was examined using reverse transcription-quantitative PCR. (C) TINCR lncRNA expression in tissues was examined using *in situ* hybridization (magnification, x200). (D) Overall survival of patients in the different groups. ***P<0.001 vs. adjacent tissues. LncRNA, long non-coding RNA; TINCR, tissue differentiation-inducing non-protein coding RNA.

level in the cervical cancer tissues was not significantly associated with age, tumor diameter, pathological type and degree of differentiation (Table II); however, it was correlated with lymph node metastasis, myometrial invasion depth and FIGO stage (P<0.05 for all; Table II).

Association between the lncRNA TINCR level and the prognosis of patients with cervical cancer. The 40 patients with cervical cancer were followed-up for 60 months. The overall 5-year survival rate of patients with a high expression of lncRNA TINCR was significantly lower than that of patients with a low expression of lncRNA TINCR (P=0.0391; Fig. 1D).

Analysis of risk factors affecting the prognosis of patients with cervical cancer. Univariate analysis demonstrated that lncRNA TINCR expression, lymph node metastasis, myometrial invasion depth and FIGO stage were all risk factors affecting the prognosis of patients with cervical cancer. Multivariate analysis demonstrated that lncRNA TINCR expression [hazard ratio (HR), 2.58; 95% CI, 1.51-4.38; P<0.05] was an independent risk factor affecting the prognosis of patients with cervical cancer (Table III).

Effect of lncRNA TINCR knockdown on the proliferation of cervical cancer cells. MTT assay revealed that the proliferation rate of HeLa and SiHa cells in the si-TINCR group decreased significantly following lncRNA TINCR knockdown (P<0.001 for both; Fig. 2A). EdU staining revealed that the number of EdU-positive HeLa and SiHa cells was significantly lower in the cells in which lncRNA TINCR was knocked down (P<0.001 for all; Fig. 2B and C).

LncRNA TINCR knockdown promotes the apoptosis of cervical cancer cells. Flow cytometry revealed that the apoptotic rate of HeLa and SiHa cells in the si-TINCR group increased significantly following lncRNA TINCR knockdown (P<0.001 for both; Fig. 2D and E). In addition, TUNEL assay confirmed that compared with that in the NC group, the number of apoptotic cells in the si-TINCR group increased significantly (P<0.001 for both; Fig. 2F and G).

lncRNA TINCR knockdown suppresses the invasion and migration of cervical cancer cells. Transwell assay confirmed that the number of invasive HeLa and SiHa cells in the si-TINCR group was significantly lower than

Table II. The relationship between the expression of lncRNA TINCR and clinicopathological characteristics in cervical cancer.

Clinicopathological parameters	N	lncRNA TINCR		χ^2	P-value
		High expression (n=20)	Low expression (n=20)		
Age, years				0.004	0.948
≤55	19	9	10		
>55	21	10	11		
Tumor diameter (cm)				0.110	0.740
≤4	16	9	7		
>4	24	11	13		
Pathological type				0.014	0.906
Adenocarcinoma	9	5	4		
Squamous cell carcinoma	31	15	16		
Differentiation degree				0.043	0.835
Moderately and well	21	11	10		
Poor	19	9	10		
Lymph node metastasis				12.546	0.000
Yes	18	14	4		
No	22	6	16		
Myometrial infiltration depth				8.154	0.001
>1/2	17	13	4		
≤1/2	23	7	16		
International Federation of Gynecology and Obstetrics stage				12.016	0.000
I-II	18	2	16		
III-IV	22	18	4		

Lnc, long non-coding; TINCR, tissue differentiation-inducing non-protein coding RNA.

Table III. Analysis of risk factors affecting the prognosis of cervical cancer patients.

Variable	Single factor analysis			Multiple factor analysis		
	Hazard ratio	95% CI	P-value	HR	95% CI	P-value
lncRNA TINCR expression	2.58	1.51-4.38	0.000	2.51	1.67-3.81	0.000
Lymph node metastasis	2.14	1.22-3.68	0.004	1.55	0.92-2.57	0.112
Depth of myometrial infiltration	3.46	2.19-5.12	0.002	1.6	0.75-3.55	0.092
International Federation of Gynecology and Obstetrics stage	2.75	1.77-4.28	0.001	1.69	0.84-3.45	0.223

Lnc, long non-coding; TINCR, tissue differentiation-inducing non-protein coding RNA.

that in the control group (P<0.001 for both; Fig. 3A and B). Wound healing assay also revealed that the wound healing rate of HeLa and SiHa cells in the si-TINCR group at 24 and 48 h was significantly decreased (P<0.01 for both; Fig. 3C and D).

mRNA expression and association between lncRNA TINCR and miRNA-7. Using RT-qPCR, it was found that compared with that in the NC group, in the HeLa and SiHa cells transfected with si-TINCR, lncRNA TINCR mRNA expression was significantly decreased and the miRNA-7 mRNA level was significantly increased (P<0.001 for both; Fig. 4 and B).

Bioinformatics analysis revealed that TINCR could target and regulate miRNA-7 (Fig. 4C). Dual-luciferase reporter assay demonstrated that following the transfection of miRNA-7 mimic into HeLa and SiHa cells in the WT-TINCR and MT-TINCR groups, the fluorescence intensity of lncRNA TINCR was significantly decreased (P<0.001 for both; Fig. 4C).

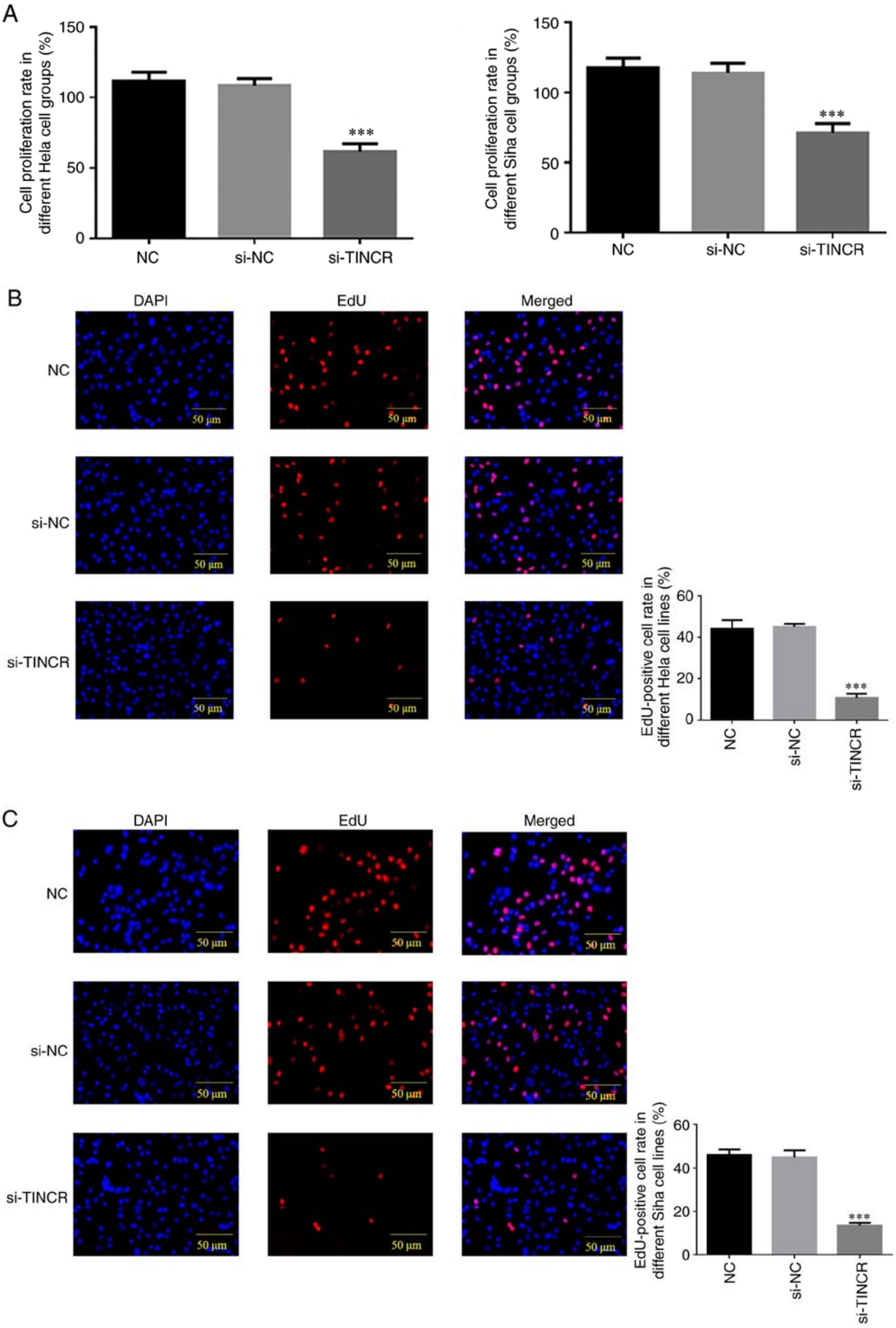

Figure 2. Continued.

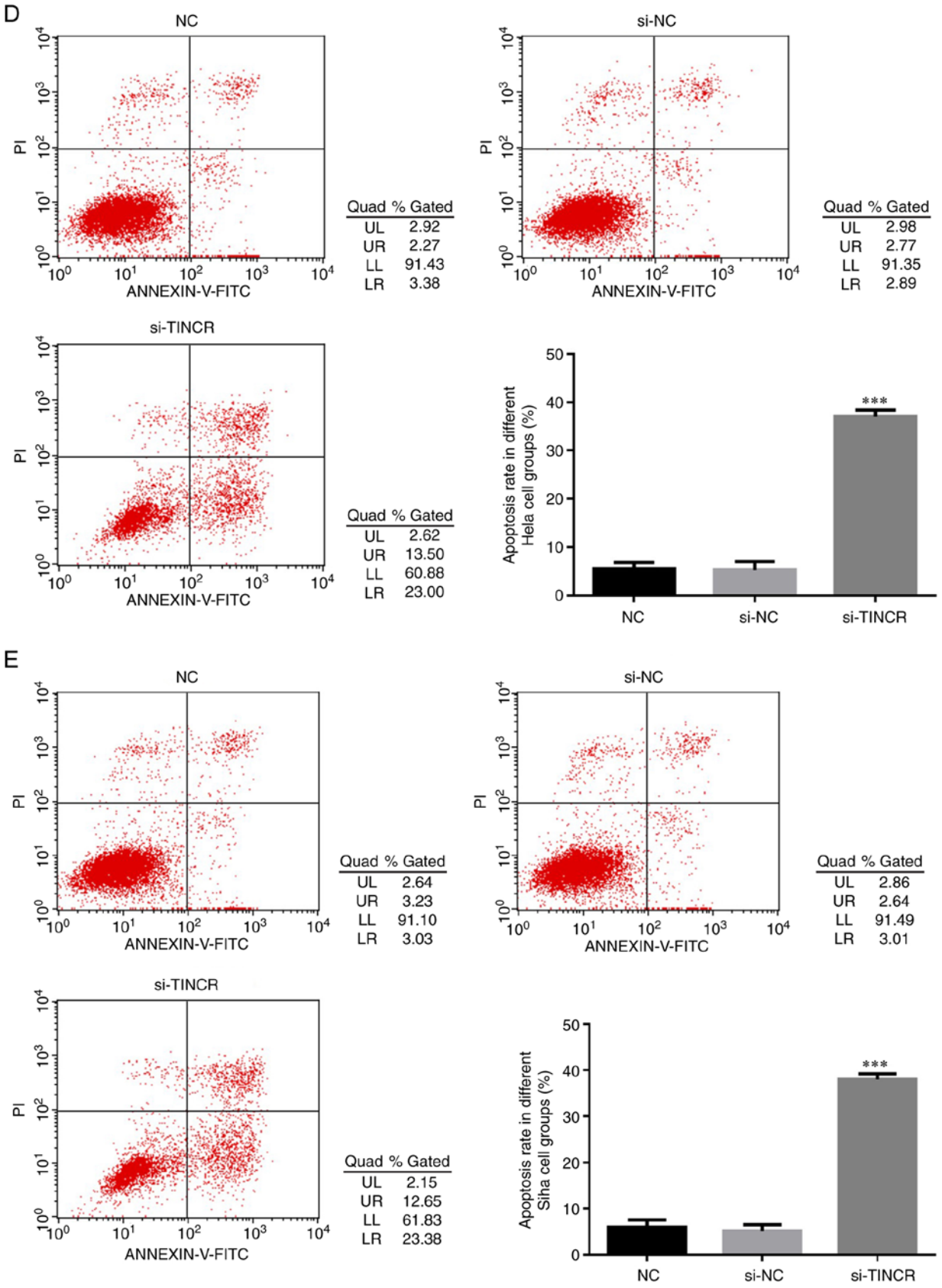

Figure 2. Continued.

Role of miRNA-7 in the inhibition of cervical cancer cell proliferation following TINCR knockdown. MTT assay revealed that the cell proliferation rate in the si-TINCR + miRNA-7 ASO group was significantly increased (P<0.001 for both; Fig. 5A) compared with that in the si-TINCR group. EdU staining demonstrated that after si-TINCR and miRNA-7

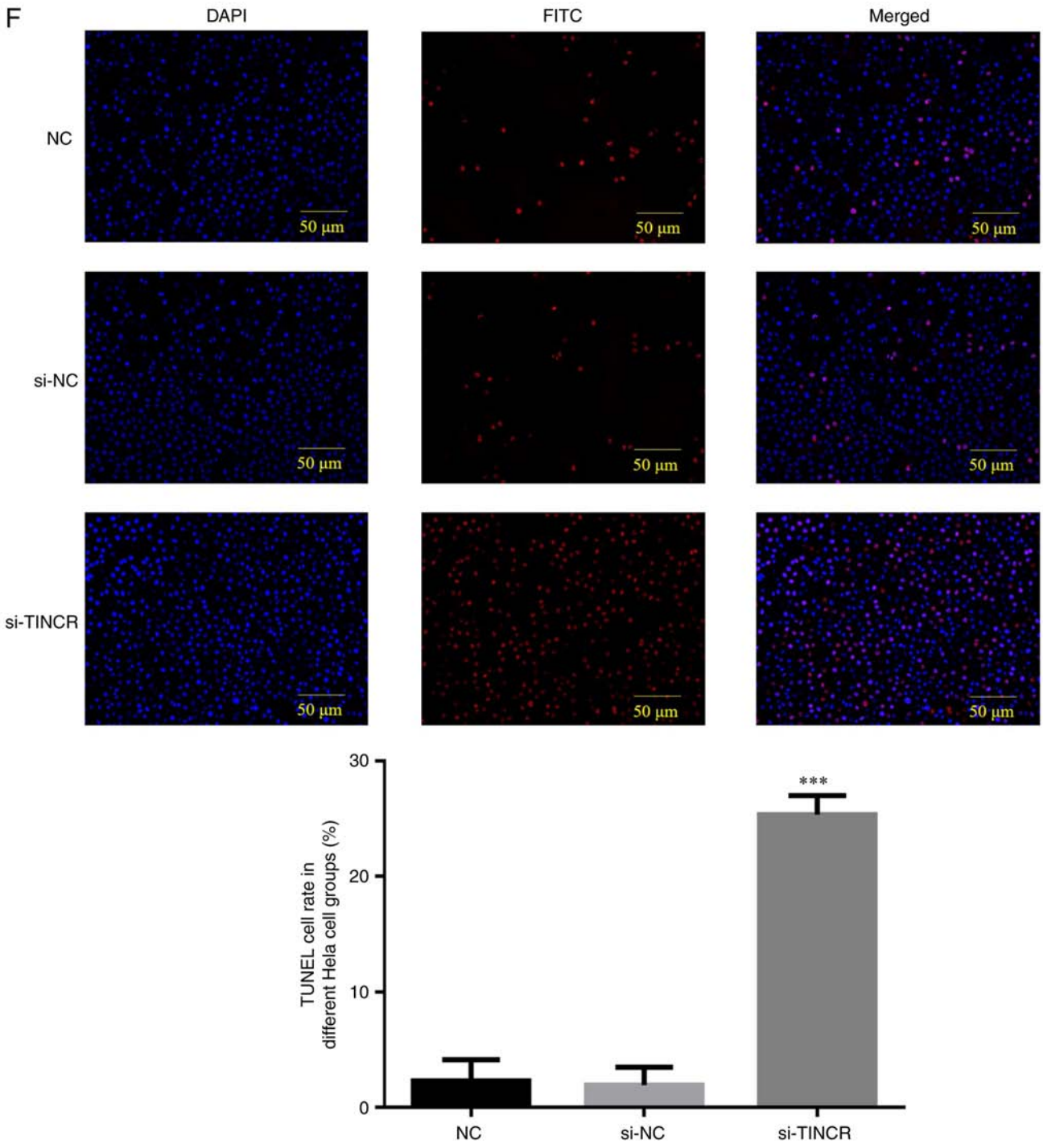

Figure 2. Continued.

ASO were co-transfected into HeLa and SiHa cells, the EdU-positive HeLa and SiHa cell number was significantly increased in the si-TINCR + miRNA-7 ASO group (P<0.001 for both; Fig. 5B and C).

Role of miRNA-7 in the promotion of cervical cancer cell apoptosis following TINCR knockdown. Flow cytometry revealed that after si-TINCR and miRNA-7 ASO were co-transfected into HeLa and SiHa cells, the apoptotic rate of the si-TINCR + miRNA-7 ASO group was significantly lower than that of the si-TINCR group (P<0.001 for both; Fig. 5D and E). TUNEL assay revealed that after si-TINCR and miRNA-7 ASO were co-transfected into HeLa and SiHa cells, the positive apoptotic cell rate of the si-TINCR + miRNA-7 ASO group was significantly decreased (P<0.001 for both; Fig. 5F and G).

Role of miRNA-7 in the inhibition of cervical cancer cell invasion and migration following TINCR knockdown. Transwell assay confirmed that after si-TINCR and miRNA-7 ASO were co-transfected into HeLa and SiHa cells, the number of invasive cells in the si-TINCR + si-miRNA group significantly increased compared with that in the si-TINCR group (P<0.001 for both; Fig. 6A and B). Wound healing

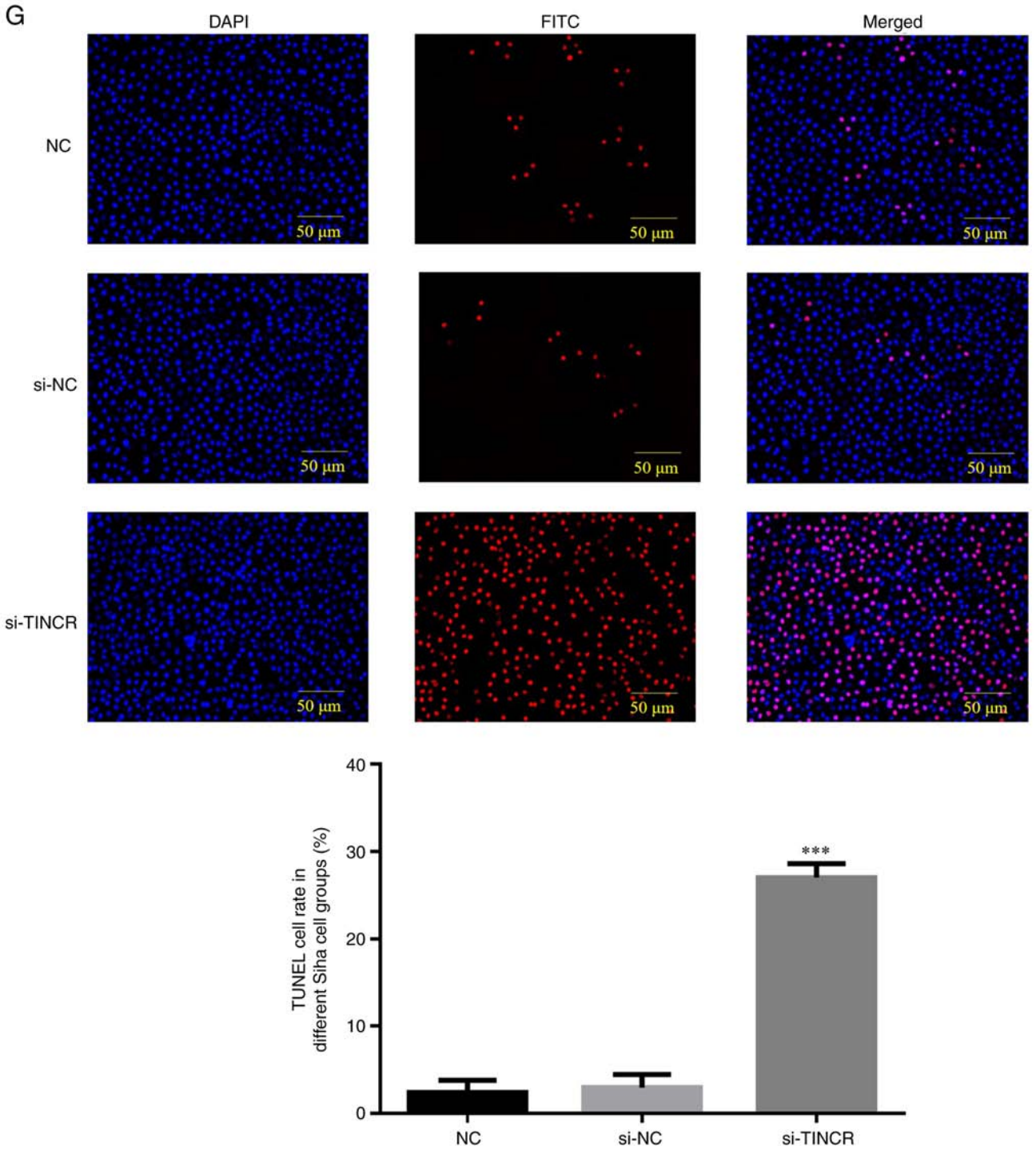

Figure 2. Effects of tissue differentiation-inducing non-protein coding RNA knockdown on the proliferation and apoptosis of cervical cancer cells. (A) Cell proliferation rate in the different HeLa and SiHa cell groups was examined using MTT assay (cell stage at 0 h as 100%). EdU-positive cell rate in different (B) HeLa and (C) SiHA cell groups (magnification, x200). Apoptotic rate of different (D) HeLa and (E) SiHA cell groups was examined using flow cytometry. TUNEL-positive rate in different (F) HeLa and (G) SiHA cell groups (magnification, x200). ***P<0.001 vs. NC group. NC, negative control group; si-, small interfering RNA; EdU, 5-ethynyl-2'-deoxyuridine.

assay revealed that after si-TINCR and miRNA-7 ASO were co-transfected into HeLa and SiHa cells, the wound healing rate of the si-TINCR + si-miRNA group increased significantly at 24 and 48 h (P<0.001 for both; Fig. 6C and D).

Expression of related genes. RT-qPCR demonstrated that after si-TINCR and miRNA-7 ASO were co-transfected into HeLa and SiHa cells, the level of miRNA-7 in the si-TINCR + miRNA-7 ASO group was significantly lower than that in the si-TINCR group, while the mRNA levels of mTOR, HIF-1α and VEGF increased significantly (P<0.001 for all; Fig. 7A and B). No significant differences were found in the mRNA level of TINCR among the three groups (P>0.05; Fig. 7A and B).

Expression of related proteins. Western blot analysis revealed that after si-TINCR and miRNA-7 ASO were co-transfected

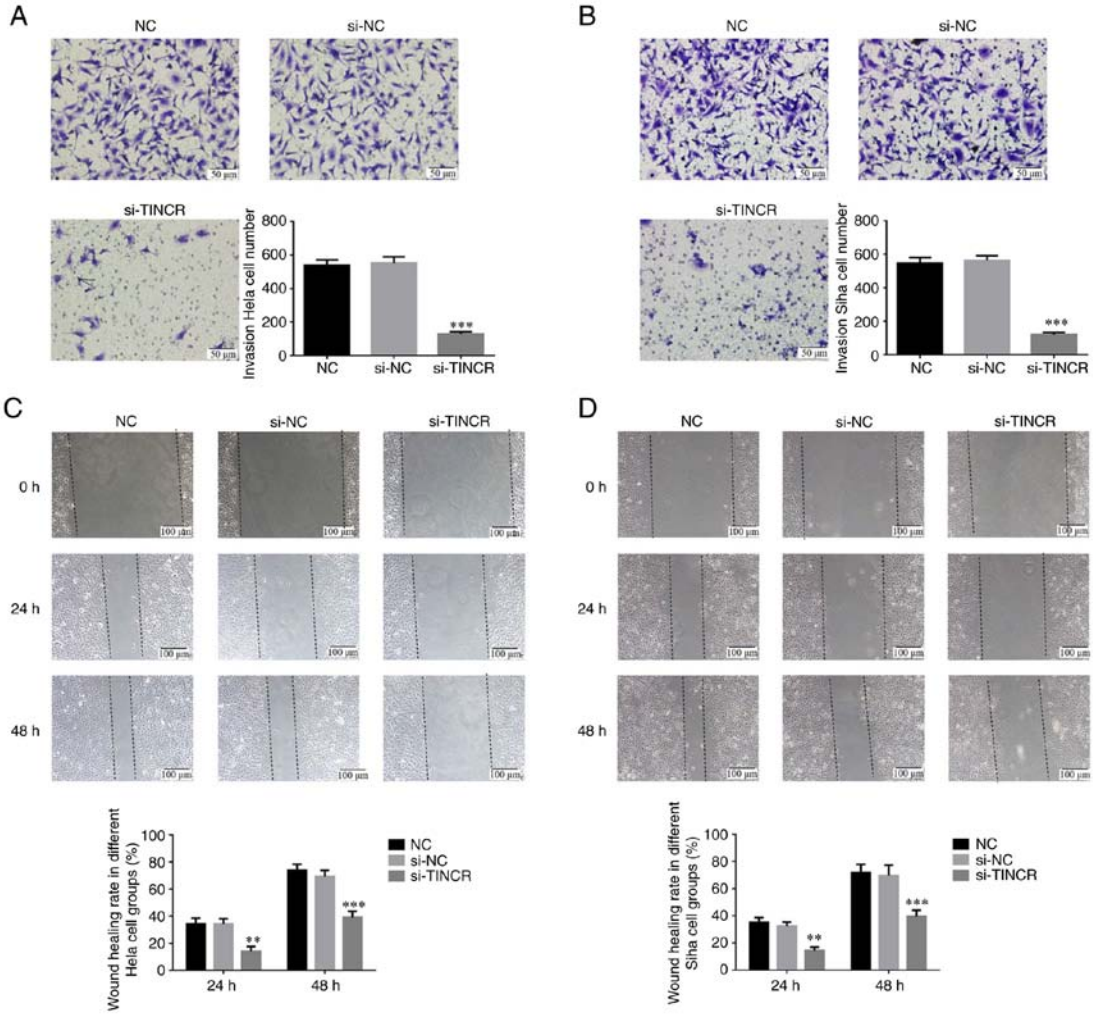

Figure 3. Tissue differentiation-inducing non-protein coding RNA knockdown inhibits the invasion and migration of cervical cancer cells. Cell invasion of (A) HeLa cells and (B) SiHA cells (magnification, x200). (C) Wound healing rate in different groups of HeLa and SiHa cells (magnification, x200). (D) Wound healing rate in different groups of SiHa cells. **P<0.01 and ***P<0.001 vs. NC group. NC, negative control group; si-, small interfering RNA.

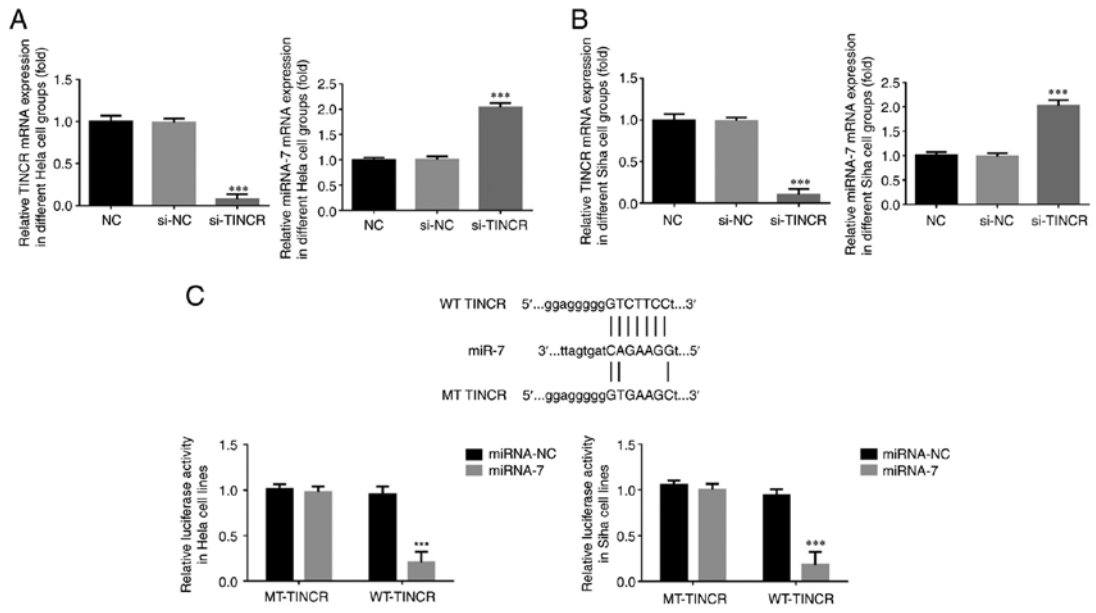

Figure 4. mRNA expression and association between lncRNA TINCR and miRNA-7. (A) LncRNA TINCR and miRNA-7 mRNA expression in the groups of (A) HeLa cell (B) SiHa cells was examined using reverse transcription-quantitative PCR. (C) Association between lncRNA TINCR and miRNA-7 expression in HeLa and SiHa cells determined using dual-luciferase assay. ***P<0.001 vs. NC group or miRNA-NC group. NC, negative control; si-, small interfering RNA; miRNA, microRNA.

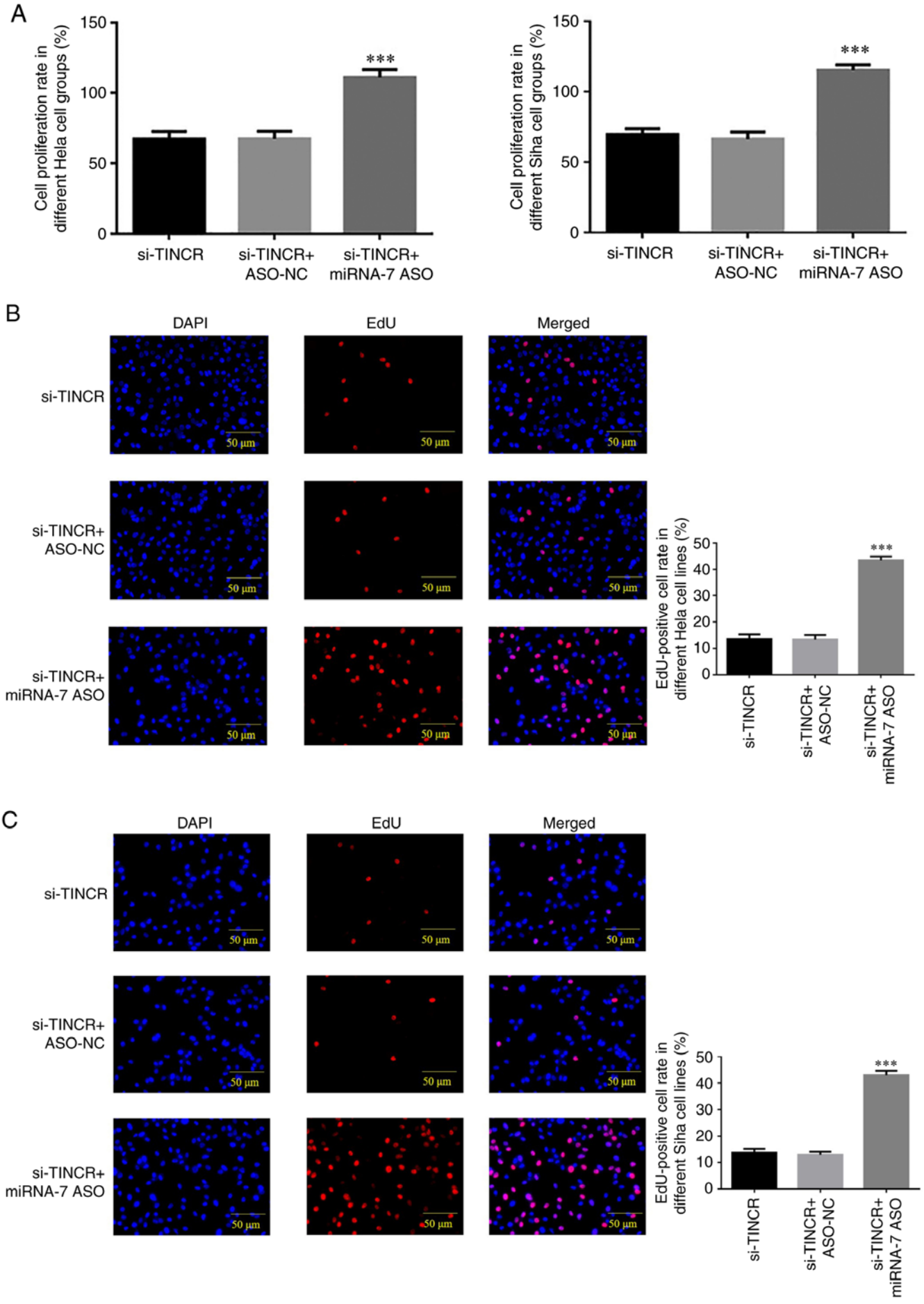

Figure 5. Continued.

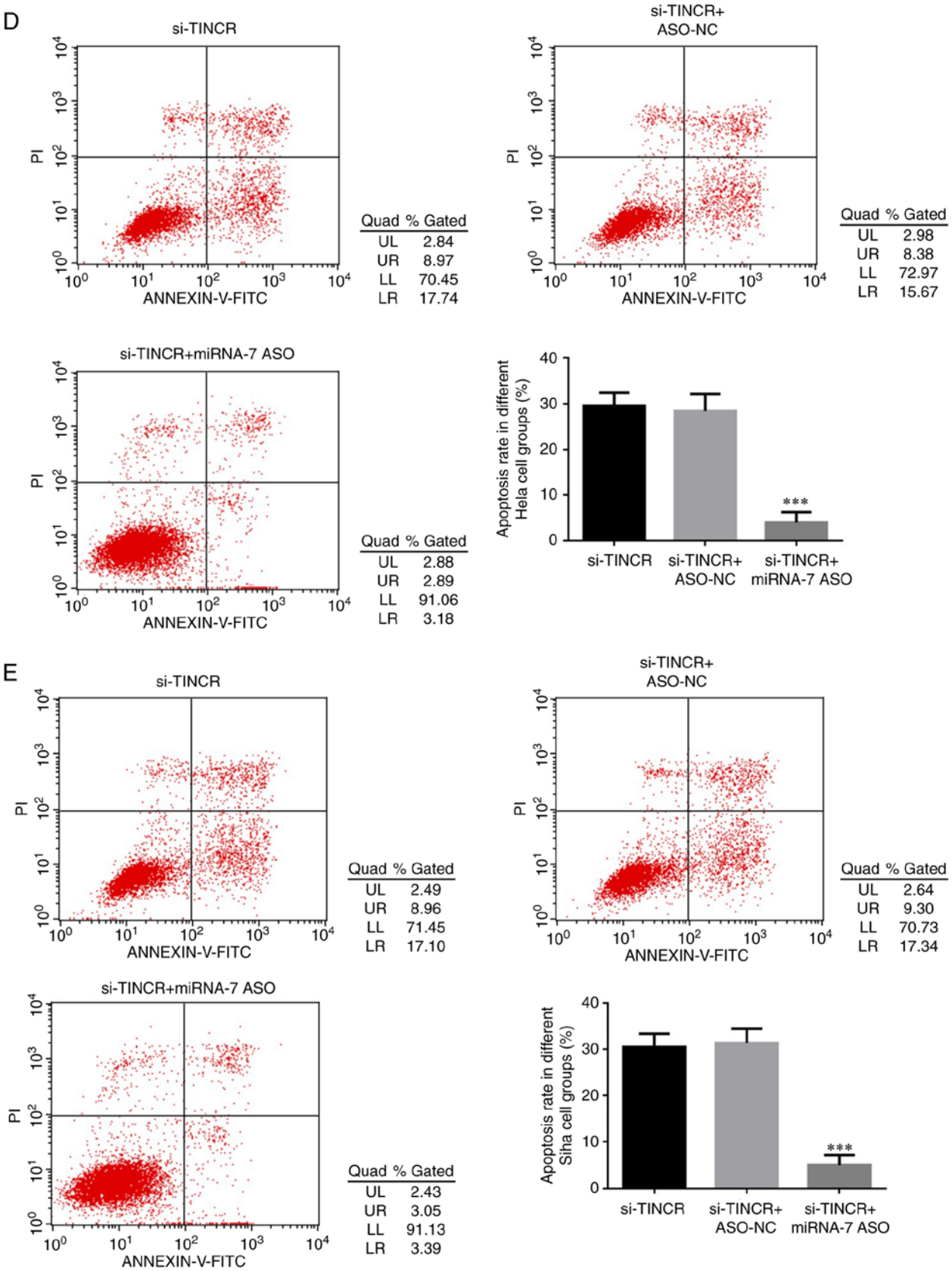

Figure 5. Continued.

into HeLa and Siha cells, the protein expression of mTOR, HIF-1α and VEGF increased significantly in the si-TINCR + miRNA-7 ASO group (P<0.001 for all; Fig. 7C and D).

Targeted regulation of mTOR by miRNA-7. Bioinformatics analysis revealed that miRNA-7 could target and regulate mTOR (Fig. 7E). Dual-luciferase reporter assay confirmed that

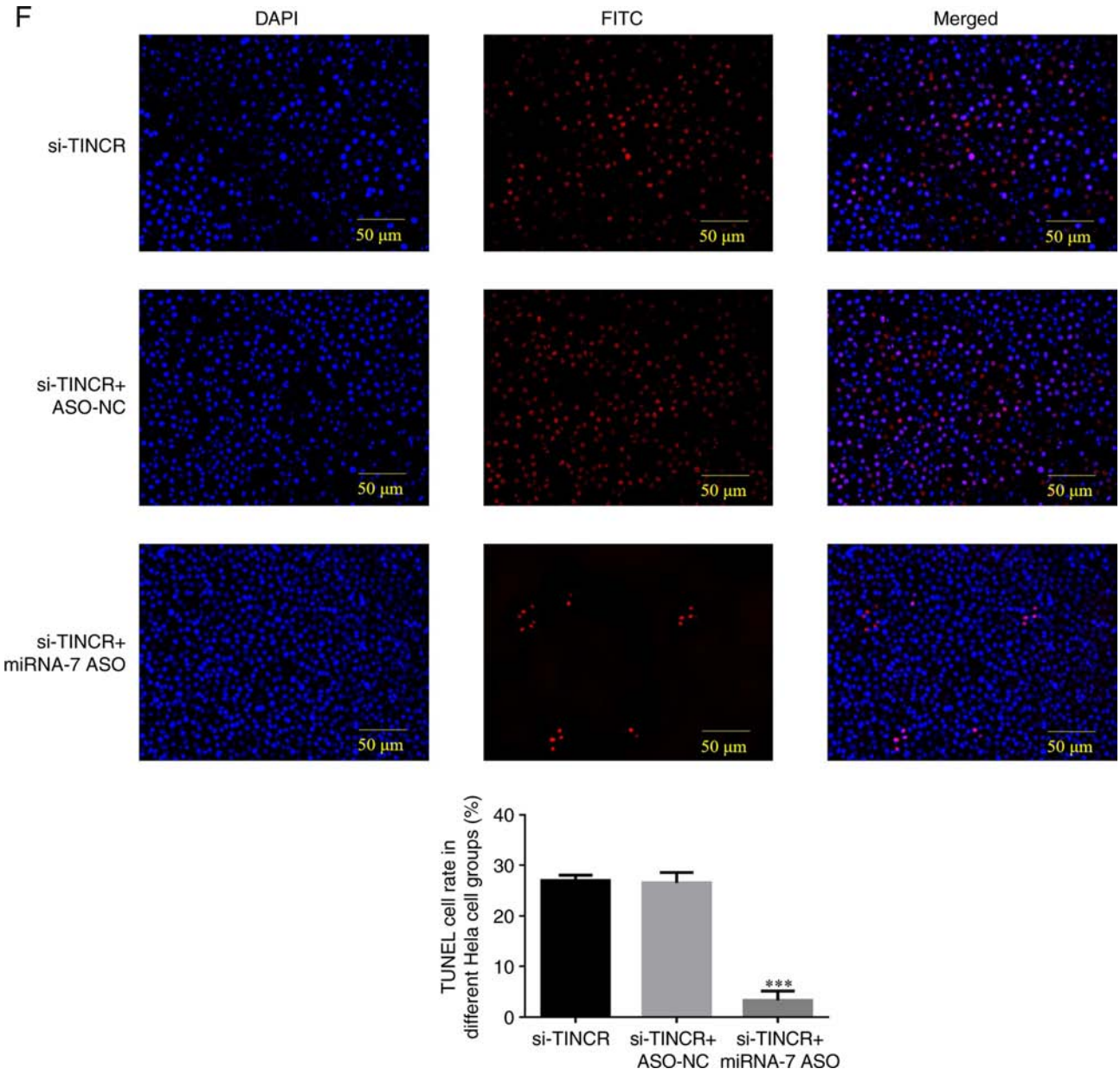

Figure 5. Continued.

in the WT mTOR group of HeLa and SiHa cells, the fluorescence intensity of the miRNA-7 group decreased significantly following the transfection of miRNA-7 into HeLa and SiHa cells ($P<0.001$ for both; Fig. 7E). In the MT mTOR group, there was no significant difference between the miRNA-NC and miRNA-7 groups ($P>0.05$).

Discussion

In the human genome, only 2% of genes can encode proteins, and non-coding RNAs account for ~98%. lncRNAs are a class of relatively long non-coding RNAs, which can regulate cell proliferation, migration, invasion and apoptosis through a variety of mechanisms, and are closely related to cancer occurrence and development (20). The majority of lncRNAs have highly conserved secondary and tertiary structures, which indicate that they can play a role in a variety of biological processes (21). lncRNAs in cervical cancer have been widely reported. TINCR has been shown to promote cell proliferation, and is involved in tumorigenesis, although it has different effects in different tumors (5,7). The expression of TINCR is upregulated in lung cancer and it is related to the clinicopathological characteristics of patients; the suppression of the TINCR level can inhibit the malignant metastasis potential of tumor cells (6). However, TINCR functions as a tumor suppressor in prostate cancer and can inhibit tumor metastasis (5). TINCR is highly expressed in liver cancer, and TINCR may be a promoter of liver cancer progression (7). The current study showed that the level of lncRNA TINCR was significantly higher in cervical cancer tissues, suggesting that lncRNA TINCR may be involved in the occurrence and development of cervical cancer. The previous studies found lncRNA TINCR as a suppressor factor in prostate cancer (5) and squamous cell carcinoma (22) and as an oncogenic factor in colorectal cancer (23). Meanwhile, the present research also found lncRNA TINCR was significantly upregulated in

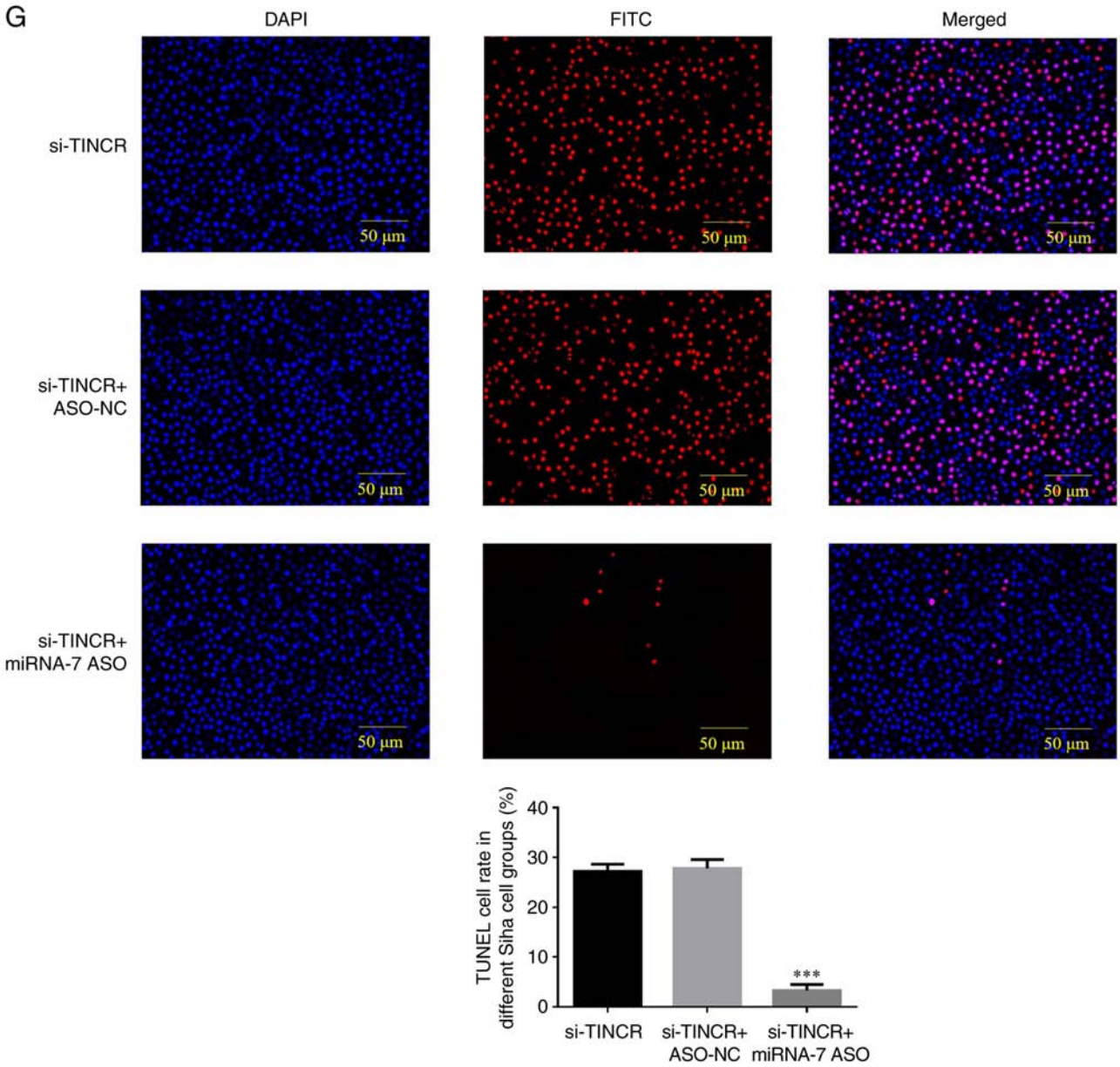

Figure 5. Role of miRNA-7 in the inhibition of cervical cancer cell proliferation caused by TINCR knockdown. (A) Cell proliferation rate in the different groups was examined using MTT assay. EdU-positive cell rate in the different groups of (B) HeLa and (C) SiHa cells (magnification, x200). Apoptotic rate of (D) HeLa and (E) SiHa cells in the different groups was examined using flow cytometry. (F) TUNEL-positive cell rate of HeLa and (G) SiHa cells in the different groups was examined using TUNEL assay (magnification, x200). ***P<0.001 vs. si-TINCR group. MiRNA, microRNA; ASO, miRNA-7 inhibitor; NC, negative control; si-, small interfering RNA; TINCR, tissue differentiation-inducing non-protein coding RNA.

cervical cancer tissues and closely correlated with poor prognosis in cervical cancer like colorectal cancer (23); however, the mechanism was different, based on the present results, with lncRNA TINCR knockdown, miRNA-7 increasing and mTOR, HIF-11α and VEGF expression decreasing. The expression of lncRNA TINCR in cervical cancer tissues was associated with lymph node metastasis, myometrial invasion depth and FIGO stage, indicating that the expression of lncRNA TINCR may affect the progression of cervical cancer. In addition, the survival curves of patients with high and low lncRNA TINCR expression at 1-60 months following surgery were drawn. The 5-year survival rate of patients with a high lncRNA TINCR expression was significantly lower than that of those with a low lncRNA TINCR expression, suggesting that a high lncRNA TINCR expression has a detrimental effect on the prognosis of patients with cervical cancer. Moreover, Cox regression analysis of lncRNA TINCR expression, lymph node metastasis, myometrial invasion depth and FIGO stage revealed that lncRNA TINCR expression, lymph node metastasis, myometrial invasion depth and FIGO stage were all risk factors affecting the prognosis of patients with cervical cancer, among which lncRNA TINCR expression was an independent risk factor affecting the prognosis of patients with cervical cancer; this suggests that the inhibition of lncRNA TINCR expression may improve the prognosis of patients with cervical cancer. To further explore the mechanisms of lncRNA TINCR in cervical cancer, lncRNA TINCR was knocked down using *in vitro* experiments, revealing that the biological

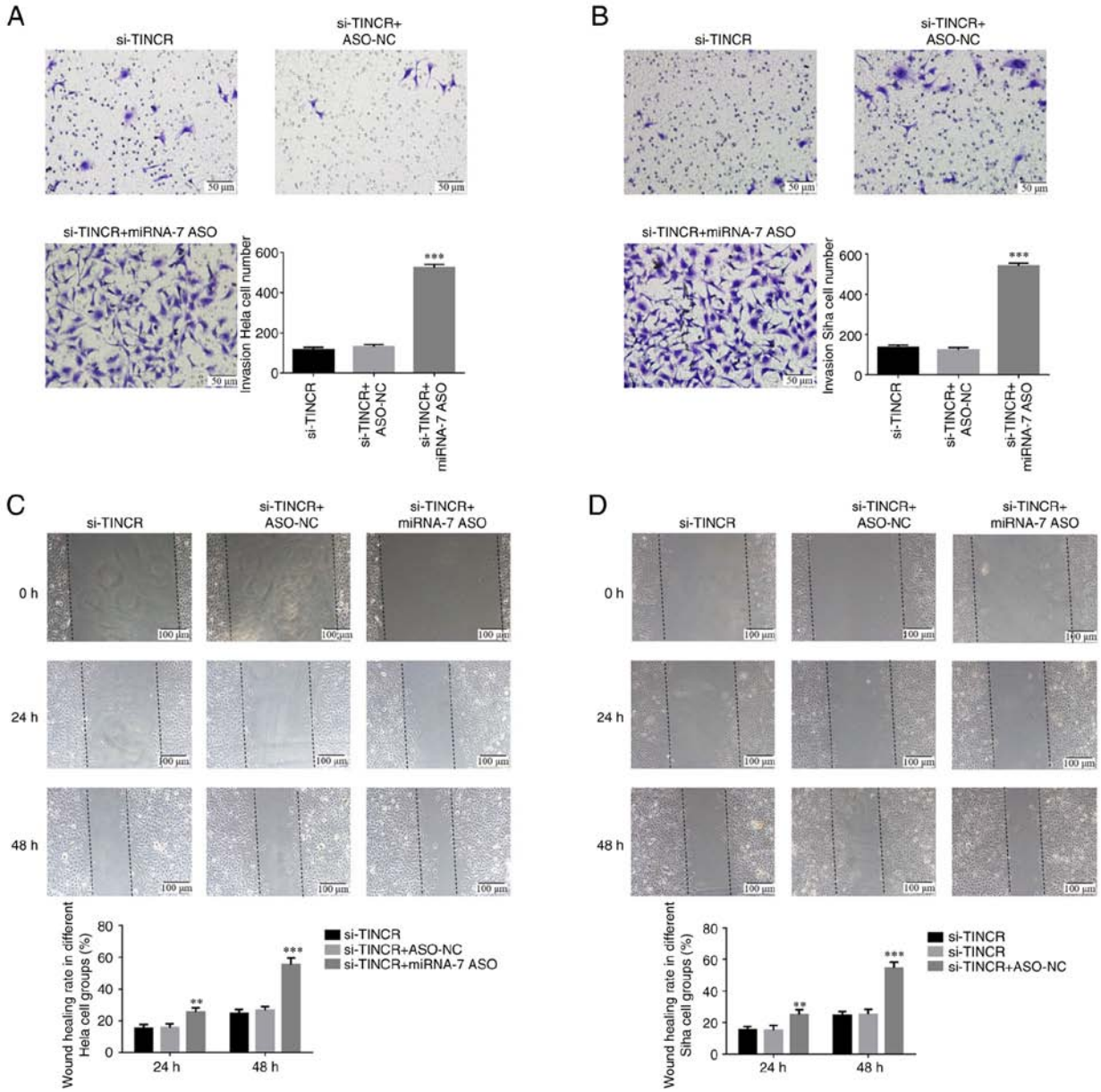

Figure 6. Role of miRNA-7 in the inhibition of cervical cancer cell invasion and migration caused by TINCR knockdown. Cell invasion of (A) HeLa and (B) SiHa cells (magnification, x200). Wound healing rate of (C) HeLa cells and (D) SiHa cells in the different groups (magnification, x200). **P<0.01 and ***P<0.001 vs. si-TINCR group. MiRNA, microRNA; ASO, miRNA-7 inhibitor; NC, negative control; si-, small interfering RNA; TINCR, tissue differentiation-inducing non-protein coding RNA.

activities (proliferation, invasion and migration) of cervical cancer cell lines Siha and Hela were significantly inhibited. The aforementioned results suggested that TINCR may play a promoting role in the progression of cervical cancer, and its knockdown can effectively inhibit the occurrence and progression of colon cancer.

Research on the mechanisms of lncRNAs revealed that lncRNAs could play different biological roles by targeting and regulating the expression of downstream genes, and the targeting and regulatory role of lncRNAs in different tissues and pathological processes may differ (24). In the present study, it was found that TINCR targeted and regulated the expression of miRNA-7 in cervical cancer cell lines. miRNA-7 is a downregulated miRNA molecule in cancer tissues, and its overexpression can inhibit the biological activities of cancer cell lines (16). Additionally, it was observed that TINCR targeted and regulated the expression of miRNA-7 in cervical cancer cell lines, and the silencing of miRNA-7 reversed the inhibitory effects of TINCR knockdown on the invasion and migration of cervical cancer cells; this indicates that the inhibitory effects of TINCR knockdown on the invasion and migration of cervical cancer cells are related to the targeted regulation of miRNA-7.

Through bioinformatics analysis, it was found that miRNA-7 could target and regulate mTOR, playing a role in inhibiting the biological activities of cervical cancer cells. mTOR is an atypical serine/threonine kinase composed of 2,549 amino acids, which is a member of the phosphatidylinositol 3-kinase-related protein kinase family (25). The mTOR signaling pathway regulates cell membrane transport, protein

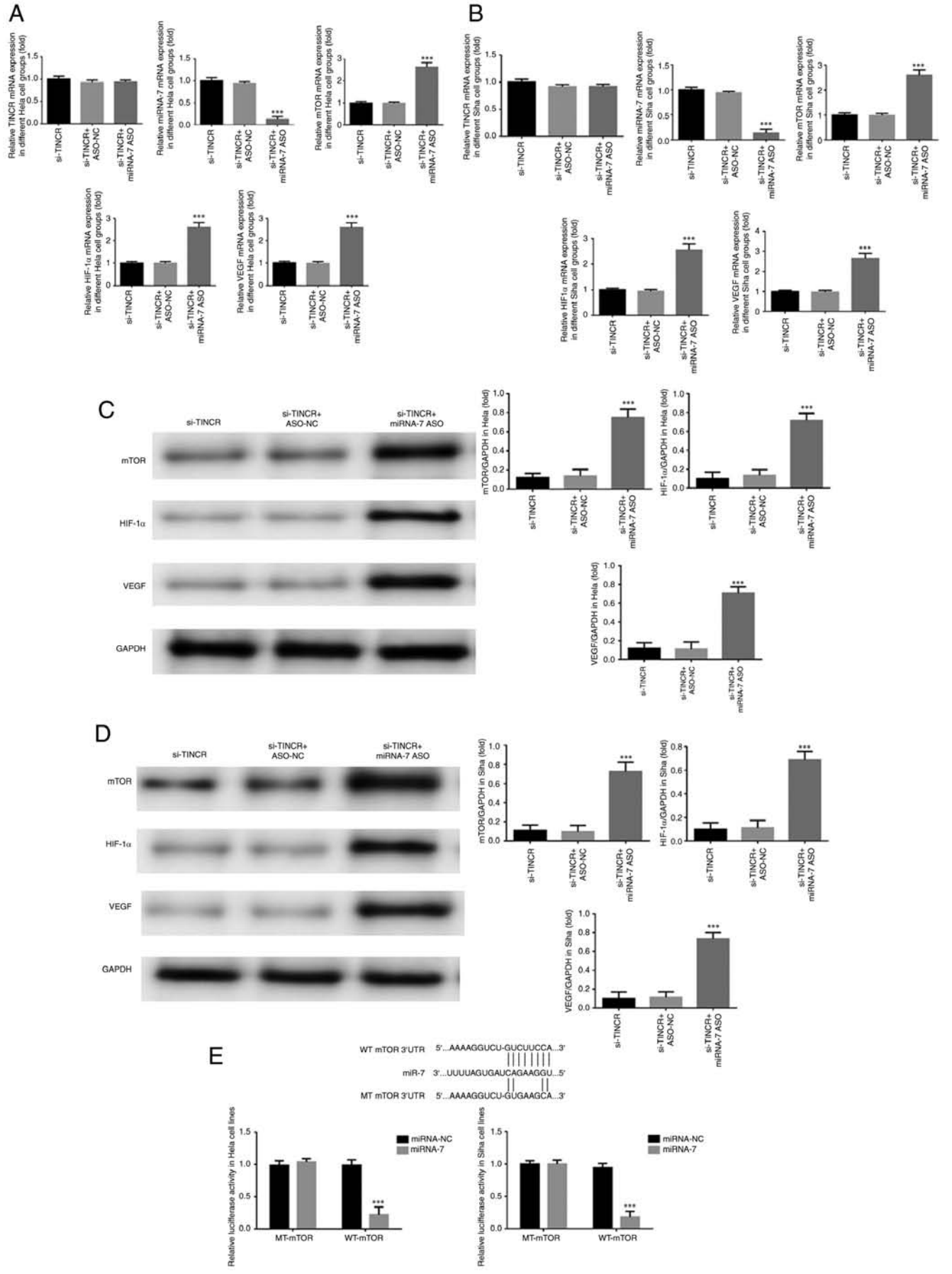

Figure 7. Expression of relevant genes and proteins, and association between miRNA-7 and mTOR. Relative mRNA expression in (A) HeLa and (B) SiHa cells in the different groups. (C) Relative protein expression of mTOR, hypoxia-inducible factor 1 subunit α and VEGF in (C) HeLa and (D) SiHa cells in the different groups was examined using western blot analysis. (E) Targeted regulation of mTOR by miRNA-7. ***P<0.001 vs. si-TINCR group. MiRNA, microRNA; ASO, miRNA-7 inhibitor; NC, negative control; si-, small interfering RNA; TINCR, tissue differentiation-inducing non-protein coding RNA.

degradation, nutritional metabolism and tumor occurrence through phosphorylation, and plays a critical regulatory role in physiological processes, including cell growth, proliferation, differentiation and apoptosis (26), it is also widely involved in biological processes, such as gene transcription, protein translation and ribosome biogenesis (27). HIF-1α is a DNA-binding protein, which is widely involved in the specific response induced by hypoxia in mammalian cells, and plays a key role in the regulation of gene expression induced by hypoxia (28). Ryan *et al* (29) first proved in 1998 that HIF-1α deletion can inhibit tumor growth and reduce the ability of tumor cell invasion and metastasis. The increased expression of HIF-1α can lead to the upregulation of numerous target genes, such as HVEGF, erythropoietin, glucose-encoding transporter, glycolytic enzyme, etc. Its activity plays a key role in maintaining the energy metabolism of tumor cells, angiogenesis, and promoting tumor proliferation and metastasis (30). EGF is a heparin-binding growth factor specific to vascular endothelial cells, with a classical signal sequence (31). VEGF can cause a series of signal transduction mechanisms by binding with receptors, promoting the release of various growth factors and cytokines, and promoting the proliferation and migration of endothelial cells, thus inducing angiogenesis *in vivo* (32). Therefore, the expression and secretion level of VEGF is one of the key indicators for the evaluation of angiogenesis. Tumor cells can overexpress VEGF, thereby accelerating angiogenesis and promoting tumor invasion and metastasis (33). The expression of EGF is regulated by the transcription factor, HIF-1α, and HIF-1α activity is regulated by mTOR; thus, mTOR is the key signaling pathway regulating VEGF expression (34). HIF-1α and VEGF are considered downstream targets of mTOR. A previous study (35) suggested that the mTOR signaling pathway can be inhibited by directly inhibiting the growth of vascular endothelial cells stimulated by VEGF. In the present study, it was found that following the knockdown of lncRNA TINCR, with the increase in miRNA-7 expression, the mTOR/HIF-1α/VEGF signaling pathway was significantly inhibited, indicating that the cancer-promoting effect of lncRNA TINCR in cervical cancer may be related to the activation of the mTOR/HIF-1α/VEGF signaling pathway caused by the decreased expression of miRNA-7.

In conclusion, the present study demonstrates that the abnormally high expression of lncRNA TINCR plays a critical role in the occurrence and development of cervical cancer. The mechanism of lncRNA TINCR in promoting carcinogenesis may be closely related to the miRNA-7/mTOR axis and the mTOR/IF-1α/VEGF signaling pathway.

Acknowledgements

Not applicable.

Funding

No funding was received.

Availability of data and materials

The datasets used and/or analyzed during the current study are available from the corresponding author on reasonable request.

Authors' contributions

TZ and XL designed the study and performed the experiments. XL revised the manuscript for important intellectual content. XL, CW and QF collected and analyzed the data. XW and QF confirm the authenticity of all the raw data. All authors read and approved the final manuscript.

Ethics approval and consent to participate

The present study was approved by the Ethics Committee of the Women and Children's Hospital, Qingdao University (approval no. 2015081305). The patient or immediate family member signed an informed consent form.

Patient consent for publication

Not applicable.

Competing interests

The authors declare that they have no competing interests.

References

1. Small W Jr, Bacon MA, Bajaj A, Chuang LT, Fisher BJ, Harkenrider MM, Jhingran A, Kitchener HC, Mileshkin LR, Viswanathan AN and Gaffney DK: Cervical cancer: A global health crisis. Cancer 123: 2404-2412, 2017.
2. Wardak S: Human Papillomavirus (HPV) and cervical cancer. Med Dosw Mikrobiol 68: 73-84, 2016.
3. Shah CA, Beck T, Liao JB, Giannakopoulos NV, Veljovich D and Paley P: Surgical and oncologic outcomes after robotic radical hysterectomy as compared to open radical hysterectomy in the treatment of early cervical cancer. J Gynecol Oncol 28: e82, 2017.
4. Schmitz SU, Grote P and Herrmann BG: Mechanisms of long non-coding RNA function in development and disease. Cell Mol Life Sci 73: 2491-2509, 2016.
5. Dong L, Ding H, Li Y, Xue D and Liu Y: LncRNA TINCR is associated with clinical progression and serves as tumor suppressive role in prostate cancer. Cancer Manag Res 10: 2799-2807, 2018.
6. Zhu ZJ and He JK: TINCR facilitates non-small cell lung cancer progression through BRAF-activated MAPK pathway. Biochem Biophys Res Commun 497: 971-977, 2018.
7. Tian F, Xu J, Xue F, Guan E and Xu X: TINCR expression is associated with unfavorable prognosis in patients with hepatocellular carcinoma. Biosci Rep 37: BSR20170301, 2017.
8. Xu J, Zeng W, Liu T, Wan Z, Yang X, Chen J and Liu F: lncRNA TINCR knockdown inhibits colon cancer cells via regulation of autophagy. Food Sci Nutr 11: 1965-1981, 2023.
9. Luo H, Xu C, Le W, Ge B and Wang T: lncRNA CASC11 promotes cancer cell proliferation in bladder cancer through miRNA-150. J Cell Biochem 120: 13487-13493, 2019.
10. Luan X and Wang Y: LncRNA XLOC_006390 facilitates cervical cancer tumorigenesis and metastasis as a ceRNA against miR-331-3p and miR-338-3p. J Gynecol Oncol 29: e95, 2018.
11. Zhao W, Geng D, Li S, Chen Z and Sun M: LncRNA HOTAIR influences cell growth, migration, invasion, and apoptosis via the miR-20a-5p/HMGA2 axis in breast cancer. Cancer Med 7: 842-855, 2018.
12. Peng CL, Zhao XJ, Wei CC and Wu JW: LncRNA HOTAIR promotes colon cancer development by down-regulating miRNA-34a. Eur Rev Med Pharmacol Sci 23: 5752-5761, 2019.
13. Thiel J, Alter C, Luppus S, Eckstein A, Tan S, Führer D, Pastille E, Westendorf AM, Buer J and Hansen W: MicroRNA-183 and microRNA-96 are associated with autoimmune responses by regulating T cell activation. J Autoimmun 96: 94-103, 2019.
14. Kara M, Yumrutas O, Ozcan O, Celik OI, Bozgeyik E, Bozgeyik I and Tasdemir S: Differential expressions of cancer-associated genes and their regulatory miRNAs in colorectal carcinoma. Gene 567: 81-86, 2015.

15. Yang Y, Li XJ, Li P and Guo XT: MicroRNA-145 regulates the proliferation, migration and invasion of human primary colon adenocarcinoma cells by targeting MAPK1. Int J Mol Med 42: 3171-3180, 2018.
16. Zeng CY, Zhan YS, Huang J and Chen YX: MicroRNA-7 suppresses human colon cancer invasion and proliferation by targeting the expression of focal adhesion kinase. Mol Med Rep 13: 1297-1303, 2016.
17. Xu N, Lian YJ, Dai X and Wang YJ: MiR-7 increases cisplatin sensitivity of gastric cancer cells through suppressing mTOR. Technol Cancer Res Treat 16: 1022-1030, 2017.
18. Chen WS, Yen CJ, Chen YJ, Chen JY, Wang LY, Chiu SJ, Shih WL, Ho CY, Wei TT, Pan HL, *et al*: MiRNA-7/21/107 contribute to HBx-induced hepatocellular carcinoma progression through suppression of maspin. Oncotarget 6: 25962-25974, 2015.
19. Livak KJ and Schmittgen TD: Analysis of relative gene expression data using real-time quantitative PCR and the 2(-Delta Delta C(T)) method. Methods 25: 402-408, 2001.
20. Tang Y, Cheung BB, Atmadibrata B, Marshall GM, Dinger ME, Liu PY and Liu T: The regulatory role of long non-coding RNAs in cancer. Cancer Lett 391: 12-19, 2017.
21. McCabe EM and Rasmussen TP: lncRNA involvement in cancer stem cell function and epithelial-mesenchymal transitions. Semin Cancer Biol 75: 38-48, 2021.
22. Morgado-Palacin L, Brown JA, Martinez TF, Garcia-Pedrero JM, Forouhar F, Quinn SA, Reglero C, Vaughan J, Heydary YH, Donaldson C, *et al*: The TINCR ubiquitin-like microprotein is a tumor suppressor in squamous cell carcinoma. Nat Commun 14: 1328, 2023.
23. Zhang X, Yao J, Shi H, Gao B and Zhang L: LncRNA TINCR/microRNA-107/CD36 regulates cell proliferation and apoptosis in colorectal cancer via PPAR signaling pathway based on bioinformatics analysis. Biol Chem 400: 663-675, 2019.
24. Zhu X, Li H, Wu Y, Zhou J, Yang G and Wang W: LncRNA MEG3 promotes hepatic insulin resistance by serving as a competing endogenous RNA of miR-214 to regulate ATF4. Int J Mol Med 43: 345-357, 2019.
25. Sehgal SN: Sirolimus: Its discovery, biological properties, and mechanism of action. Transplant Proc 35 (3 Suppl): 7S-14S, 2003.
26. Wiederrecht GJ, Sabers CJ, Brunn GJ, Martin MM, Dumont FJ and Abraham RT: Mechanism of action of rapamycin: New insights into the regulation of G1-phase progression in eukaryotic cells. Prog Cell Cycle Res 1: 53-71, 1995.
27. Edinger AL and Thompson CB: Akt maintains cell size and survival by increasing mTOR-dependent nutrient uptake. Mol Biol Cell 13: 2276-2288, 2002.
28. Semenza GL: HIF-1 mediates metabolic responses to intratumoral hypoxia and oncogenic mutations. J Clin Invest 123: 3664-3671, 2013.
29. Ryan HE, Lo J and Johnson RS: HIF-1 alpha is required for solid tumor formation and embryonic vascularization. EMBO J 17: 3005-3015, 1998.
30. Li L, Qu Y, Li J, Xiong Y, Mao M and Mu D: Relationship between HIF-1alpha expression and neuronal apoptosis in neonatal rats with hypoxia-ischemia brain injury. Brain Res 1180: 133-139, 2007.
31. Chen Y, Peng GF, Han XZ, Wang W, Zhang GQ and Li X: Apoptosis prediction via inhibition of AKT signaling pathway by neogrifolin. Int J Clin Exp Pathol 8: 1154-1164, 2015.
32. Kigure W, Fujii T, Sutoh T, Morita H, Katoh T, Yajima RN, Yamaguchi S, Tsutsumi S, Asao T and Kuwano H: The association of VEGF-C expression with tumor lymphatic vessel density and lymph node metastasis in patients with gastric cancer and gastrointestinal stromal tumor. Hepatogastroenterology 60: 277-280, 2013.
33. Lugano R, Ramachandran M and Dimberg A: Tumor angiogenesis: Causes, consequences, challenges and opportunities. Cell Mol Life Sci 77: 1745-1770, 2020.
34. Li W, Petrimpol M, Molle KD, Hall MN, Battegay EJ and Humar R: Hypoxia-induced endothelial proliferation requires both mTORC1 and mTORC2. Circ Res 100: 79-87, 2007.
35. Tsai SY, Yang LY, Wu CH, Chang SF, Hsu CY, Wei CP, Leu SJ, Liaw J, Lee YH and Tsai MD: Injury-induced Janus kinase/protein kinase C-dependent phosphorylation of growth-associated protein 43 and signal transducer and activator of transcription 3 for neurite growth in dorsal root ganglion. J Neurosci Res 85: 321-331, 2007.